Design and Optimization of Free-Fall Electrostatic Separators for Plastics Recycling

Jing Wei and Matthew J. Realff
School of Chemical and Biomolecular Engineering, Georgia Institute of Technology, Atlanta, GA 30332

Electrostatic separation is a promising technique for separating a mix of plastics, which can acquire different sign charges through triboelectrification. A particular application of growing importance is the separation of plastics with overlapping densities from a waste stream of electronic products. Particle charging, which plays an important role in separation efficiency, has been the topic of much research. However, no systematic method has been proposed for design and optimization of the separation process itself, a gap that this research seeks to fill. The aim is to compare several design options for free-fall electrostatic separators, taking into account the distribution of the particle charge and initial position. Particle trajectory and recovery models are derived under a set of simplifying assumptions that are carefully analyzed. Optimization models are developed that trade off the strength of the electric field with the size and number of stages of the free-fall separator. Several different configurations are optimized and compared under various conditions (mean value and standard deviation of particle charges, feed rate, and product prices). Finally, a general guide is proposed for selecting an appropriate design.

Introduction

Recycling is an important component of environmental protection, particularly for electronic products, where the release of toxics such as lead and mercury through incinerator ash or landfill leachate is of concern. Engineering plastics from a large fraction of electronic products are chosen as raw materials for their specific properties, design flexibility, and contribution to low manufacturing costs. It is the very fact of their low cost that makes them economically unattractive to recover, and, hence, provides incentive to synthesize low-cost recovery processes from innovative unit operations. Electrostatic separation provides many advantages over other separation methods (such as froth flotation and sink-float separation)—low energy consumption, a dry process, independence of particle shape—and it is often simpler, cheaper, and easier to control than froth flotation and other wet-medium techniques. Therefore, it is a very important separation operation whose design should be treated systematically to explore its full potential.

Correspondence concerning this article should be addressed to M. J. Realff.

When two different plastics come into contact and are subsequently separated, electrons are transferred from one to the other. Thus, different particles acquire opposite charges and can be separated in a high voltage field (usually 30–60 kV). In general, particles with a higher dielectric constant are charged positively against particles with a lower constant. Table 1 shows the relative triboelectric charging sequence of common plastics. It should be pointed out that the relative positions of plastics in the sequence depend on the experimental condition, hence the table is only for general reference. For further details about the basics of triboelectrification, readers may refer to Lowell and Rose-Innes (1980), Inculet (1984), Botsch and Köhnlechner (1997), and Kwetkus (1998).

Besides the electric properties of the materials, the triboelectric charging process can be influenced by many other factors, such as the frequency of collision (contact), humidity, material ratios, and pretreatment. Kamptner et al. (1997) demonstrated several successful examples of using surfactants. It has been shown that it is possible to change the

Table 1. Triboelectric Series of Plastics

Material	PUR	POM	PC	PA	ABS	PS	PE	PP	PET	PVC	PVDF
Series		+								−	

Source: (Stahl and Beier, 1997).

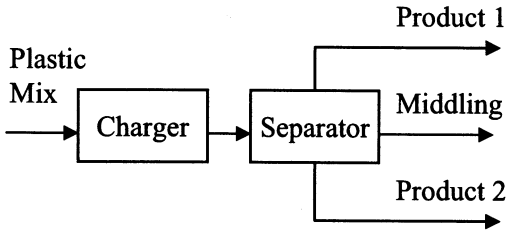

Figure 1. Separation process.

charge sign of PE in the mixture of PVC/PE/PS by surface treatment, while the sign of PVC and PS charging remains unchanged. Since the charging is affected by so many factors, the charges carried by the particles are difficult to predict. Lowell (1980) found that the standard deviation is about one-third of the mean, even to the extent that wrong sign charges are seen. It appears that a wide charge distribution may be fundamental to insulator charging, and must be accounted for in any design procedure.

Figure 1 shows the separation process. First a plastic mix is charged in a charging device and then is fed to the separator, which usually has several bins to collect the products and middling. Due to the various factors we just mentioned that might have influence on the charging process, it is reasonable to assume that different types of plastic particles have normal charge distributions with their respective mean and variance.

There are several methods of contacting particles together to generate triboelectric charging. Commonly used devices are an inclined rotating drum (Inculet et al., 1998), fluidized bed (Inculet et al., 1998), cyclone (Yanar and Kwetkus, 1995), and vibrating feeder (Higashiyama et al., 1997). For the separation process after charging, free-fall between two plates or a rotating drum are the most common designs. The free-fall design is simpler, eliminating moving parts. However, a rotating drum might be able to provide a higher throughput. Table 2 summarizes the features (single- or multistage, any conditioning, free-fall or drum type, charging method, and the materials) of experiments that have been carried out and reported in the open literature.

There are few articles that address the modeling and design of electrostatic separators. Vlad et al. (2000) modeled the behavior of charged conductive particles in plate-type (a single inclined plate with particles sliding down) electrostatic separator. The detachment points of particles were simulated and the detachment voltage at a fixed point was calculated and verified by experiments. Mihailescu et al. (2000) demonstrated a computer-assisted experimental design for optimizing the separation process. Most of the previous research on modeling electrostatic separation processes focused on single-particle behavior, instead of the overall separation efficiency (such as recoveries and grades of the products). A model-based design and optimization procedure would be helpful as a guide to the preliminary design, which could then be verified by experiments. The aim of this article is to present a systematic method that can be used to design and optimize an electrostatic separator system. The system should distinguish among several design options (single or two-stage, with or without recycle, and so on). For this purpose, unit separation models for each design option were developed. These were then used within the nonlinear optimization procedure to find optimized designs. The rest of the article is

Table 2. Summary of Literatures on Electrostatic Separation of Plastics

	M. Stage	Cond.	F/D	Charging	Materials
Yanar and Kwetkus (1995)	1 stage	No	F	Copper-lined cyclone	PVC/PE
Botsch and Köhnlechner (1997)	3 stages 2 stages	No	D	Rotating drum	Car dashboards (ABS-PC/ PVC), bottles(PET/PVC)
Kamptner et al. (1997)	2 stages	Yes	F	Vibratory feeder, mixing drum, fluidized bed	Cable(PVC/EPDM/PE), PVC/PE/PS, PVC/PET
Stahl (1997)	Multiple	Yes	F	Unknown	PP-EPDM/PA, PVDF/acetal, cable plastics(PVC/EPDM/VPE), bottles(PET/PVC)
Inculet (1998)	1 stage	No	F	Fluidized bed, rotating tube	PVC/PET, PP/HDPE
Xiao (1999)	Multiple	No	F	Rotating drum	ASR(PP/PE), ESR, refrigerators (ABS/HIPS), Bottles (PC/PVC)

M. Stage: multistage; Cond.: conditioning; F/D: free-fall or drum.

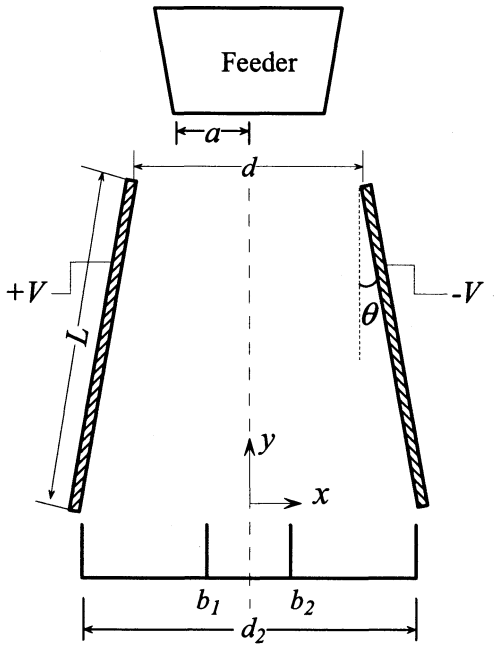

Figure 2. A free-fall electrostatic separator.

organized as follows: in the next section, we develop the trajectory model for free-fall electrostatic separators; in the third section, we first present four design options and then develop a recovery model for each design; in the fourth section, four designs are optimized and compared, and the fifth section concludes the article.

A Trajectory Model of Free-Fall Electrostatic Separators

A free-fall electrostatic separator is shown in Figure 2. The two plates, with feed gap d, end gap d_2, and length L, are inclined at angle θ and charged at constant voltage $\pm V$. Particles enter the electrical field from a feeder with feeding gap $2a$, hence the initial position of a particle is a random variable with uniform distribution $U(-a, a)$. Three collection bins (two side bins for the products and one middle bin for the middling) are placed at the bottom with the separating positions b_1 and b_2 as indicated in the figure. First, we describe the assumptions that have been used to develop the trajectory model.

Assumptions

(1) Pairwise particle–particle interaction (Coulomb force) is negligible. This is supported by the following quick calculation: for two particles with the same diameter (5 mm) and the same charge ($7.2e-10$ C) in an electrical field (4×10^5 V/m), the pairwise particle–particle interaction is 1.35 μN, which is insignificant compared to the average electrostatic force of 288 μN.

(2) Air drag force is negligible. For a spherical particle with density 1,100 kg/m^3 and dia. 5 mm in the air with density 1.2 kg/m^3 and viscosity $1.8e-5$ Pa·s, a numerical calculation showed that the differences of the time for particles to hit the bottom with or without drag force is only 0.015 s, which generates a difference in the particle horizontal position at the bottom of only 0.3 cm. For flat pieces, with a length-to-width ratio less than 2.0, the drag coefficient in the turbulent region is approximately 1.15 and the difference in the horizontal position is less than 2.4 cm, which is also not large enough to generate significant error. Therefore, this assumption is justified.

(3) Interparticle collisions are negligible. A simple Monte Carlo simulation showed that the interparticle collisions have insignificant influence on the recoveries. First, the average number of particles in the separator was computed based on the mass-flow rate and the residence time of particles in the separator. These stationary particles were uniformly distributed and placed at the center of each cell. One positive particle with random charge and initial position was allowed to fall and move toward the right-side bin. 20,000 such samples were generated, and the procedure was repeated 10 times. If during its travel, the perpendicular distance of any stationary particle to the trajectory of the moving particle was less than 1.1 of the particle diameter, there was a collision and the position was recorded. It turned out that, for a mass flow rate of 1,000 kg/h, mean particle charge (mass-to-charge ratio) of 3.0 μC/kg, and a standard deviation of 0.4, there were an average of 19,158 collisions. However, most of them are ineffective with regard to changing the final classification of the particles for the following reasons:

(a) There are an average of 1,348 collisions in region I (space above the left-side bin), which are negligible because the positive moving particle has very small velocity, so the collision has little effect on its trajectory.

(b) There are an average of 11,247 collisions in region III (space above the right-side bin), which are mostly negligible because the positive particle collides mostly with another positive particle, which does not change the classification of both particles.

(c) There are an average of 6,563 collisions in region II (space above the middle bin). Assume half of the collisions are between a positive particle and a positive particle, and the other half between a positive particle and a negative particle. Again, the collisions between two positive particles do not change their final classifications. Assuming an elastic collision between a positive particle and a negative particle, the positive moving particle absorbed the velocity of the negative particle after collision. The simulation showed that on average only 1,083 changed the classification of the positive particle (from the right-side bin to the middle or even the left-side bin).

Therefore, only 5.6% (1,083/19,158) of the total collisions affects the recoveries. The percentage is reduced as the flow rate decreases and mean charge increases. This simulation ignores the real particle distribution in the separator and the effect of collisions on this distribution, and, thus, represents a first-order attempt to characterize the effect of the collisions.

(4) Plate inner walls are inelastic, hence particles drop to the side bins after impinging against the walls. This assumption is supported by industrial practice. Some industrial designs used box electrodes consisting of a perforated plate and

a solid back plate (Yan et al., 2001) or parallel tubular electrodes (Norbert and Ingo, 1997), so that the particles can pass through after reaching the walls.

(5) Edge effects of the electrical field are negligible, which implies that the plate width and length are both sufficiently large to confine fringing effects to a small portion of the separation.

(6) The plate height is much longer than the plate gap, that is, $L \cdot \cos\ \theta \gg d$.

(7) The total charge on the particles is negligible, that is, the presence of the particles does not change the electric field. This is supported by the calculations of assumption 1.

Since the air drag force is negligible, the separation process is independent of particle size and shape, with the gravitational and electrostatic forces both proportional to the particle mass. The preceding assumptions enable a reasonably simple, analytical model of the particle trajectory to be derived and used in a design model. The translation of the single-particle trajectory model into a recovery model is carried out through a probabilistic argument based on the random variables of particle charge and initial position.

Model derivation

The potential is related to the charge density by Poisson's equation

$$\nabla^2\varphi = -\frac{\rho_c}{\epsilon_0} \tag{1}$$

and the electric field is related to the electric potential as follows

$$E = -\nabla\varphi \tag{2}$$

Based on assumption 7, in a charge-free region between two plates, Eq. 1 becomes the Laplace equation in the two-dimensional (2-D) space

$$\frac{\partial^2\varphi}{\partial x^2} + \frac{\partial^2\varphi}{\partial y^2} = 0 \tag{3}$$

By assumption 6, the second term of the preceding equation can be dropped, since it is much smaller than the first term and the model is simplified to an ODE

$$d^2\varphi/dx^2 = 0 \tag{4}$$

After scaling $\tilde{x} = x/(L\cos\theta)\tilde{y} = y/(L\cos\theta)$ and defining $\gamma = d/(L\cos\theta)$, which is the ratio of feed gap to plate height, the plate positions were determined as

$$\tilde{x}_L = -\frac{\gamma}{2} - (1-\tilde{y})\tan\ \theta, \qquad \tilde{x}_R = \frac{\gamma}{2} + (1-\tilde{y})\tan\ \theta \tag{5}$$

So, the boundary values to Eq. 4 are

$$\tilde{\varphi}|_{\tilde{x}=\tilde{x}_R} = -1 \quad \text{and} \quad \tilde{\varphi}|_{\tilde{x}=\tilde{x}_L} = 1 \tag{6}$$

The solution to Eqs. 4 and 6 is

$$\tilde{\varphi} = \frac{-\tilde{x}}{\frac{\gamma}{2} + (1-\tilde{y})\tan\ \theta} \tag{7}$$

and

$$\tilde{E}_x = -\frac{\partial\tilde{\varphi}}{\partial\tilde{x}} = \frac{1}{\frac{\gamma}{2} + (1-\tilde{y})\tan\ \theta} \tag{8}$$

In the x-direction, by Newton's second Law and scaling $\tilde{t} = t/\sqrt{2L\ cos\ \theta/g}$, we have

$$\begin{cases} \dfrac{d^2\tilde{x}}{d\tilde{t}^2} = \dfrac{2A}{1+B\tilde{t}^2} \\ \tilde{x}|_{\tilde{t}=0} = \tilde{x}_0 \quad \text{and} \quad \tilde{x}'|_{\tilde{t}=0} = 0 \end{cases} \tag{9}$$

There are two dimensionless parameters: $A = ((2V/d)q)/(mg)$, which is the ratio of electrostatic force to the gravitational force, and $B = 2\tan\ \theta/\gamma$, which is the ratio of the gap increment (equals 0 for two parallel plates) at the bottom to the feed gap. The term $1/(1+B\tilde{t}^2)$ represents the ratio of the feed gap to the gap at the particle position. The solution to Eq. 9 is

$$\tilde{x} = \tilde{x}_0 + 2\frac{A}{B}\left[\sqrt{B}\,\tilde{t}\arctan\sqrt{B}\,\tilde{t} - \ln\sqrt{1+B\tilde{t}^2}\right] \tag{10}$$

Since $\tilde{t} = \sqrt{1-\tilde{y}}$, the particle trajectory is

$$\tilde{x} = \tilde{x}_0 + 2\frac{A}{B}\left[\sqrt{B(1-\tilde{y})}\arctan\sqrt{B(1-\tilde{y})} - \ln\sqrt{1+B(1-\tilde{y})}\right] \tag{11}$$

and the particle position at the bottom is

$$\tilde{x} = \tilde{x}_0 + 2\frac{A}{B}\left[\sqrt{B}\arctan\sqrt{B} - \ln\sqrt{1+B}\right] \tag{12}$$

For two parallel plates ($\theta = 0$ and $B = 0$), the particle trajectory is

$$\tilde{x} = \tilde{x}_0 + A(1-\tilde{y}) \tag{13}$$

and the particle position at the bottom is

$$\tilde{x} = \tilde{x}_0 + A \tag{14}$$

Now that we have the equation for particle position at the bottom as a function of the initial position, particle charge, and electrostatic design variables, we are ready to derive the recovery model, which is presented in the next section.

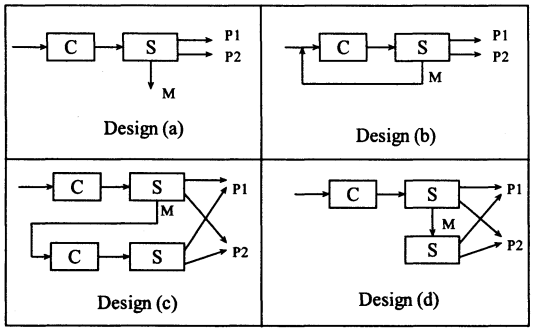

C: Charging device; S: separator; P1, P2: products; M: middling

Figure 3. Four design options.

The Recovery Model of the One-Stage and Two-Stage Free-Fall Electrostatic Separators

One of the objectives of this article is to compare the following design options (Figure 3):

(a) One-stage without recycle;

(b) One-stage with recycle (middling is sent back to the charging device and recharged);

(c) Two-stage with recharge (middling of the first stage is sent to the second stage after recharging);

(d) Two-stage without recharge (middling of the first stage is sent to the second stage for separation directly).

Recovery models need to be derived for this purpose. The problem is stated as: Given a separator, the particle charge distribution and the distribution of the entering position, what would be the recovery of each type of particle in each bin? The particle charge-to-mass ratio q_m is assumed to be normally distributed with mean μ and standard deviation σ, and the particle entering position x_0 is assumed to be uniformly distributed within $(-a, a)$. Once the recovery model for option (a) is derived, the derivation for option (b) or (c) is straightforward, assuming for option (b) that the recycled portion has the same distribution as the fresh feed after recharging and for option (c) that the feed to the second stage has the same distribution as the feed to the first stage. However, for option (d), the model is more complicated, because the feed to the second stage has different distribution from the feed to the first stage. Next, we derive the recovery models for designs (a) and (d).

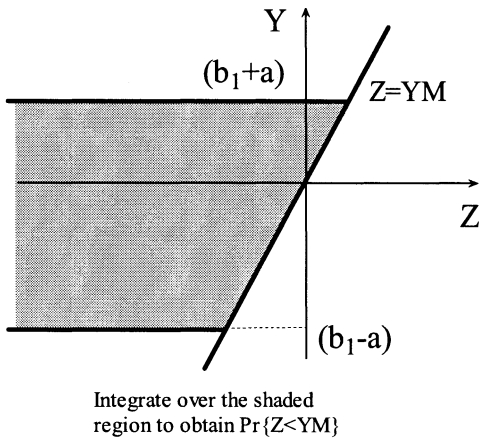

Figure 4. Probability of one random variable less than a function of another random variable.

The recovery model for design a

The recovery of any type of particles to the left-side bin equals the probability of the particle position at the bottom being less than b_1, that is, $\Pr\{x < b_1\}$, which is a function of the initial position by Eq. 12

$$\Pr\left\{x_0 + \frac{2Vq}{mg\tan\theta}\left[\sqrt{B}\arctan\sqrt{B} - \ln\sqrt{1+B}\right] < b_1\right\} \quad (15)$$

Define

$$M = \begin{cases} \dfrac{1}{\dfrac{2V}{g\tan\theta}\left[\sqrt{B}\arctan\sqrt{B} - \ln\sqrt{1+B}\right]}, & \theta > 0 \\ \dfrac{gd}{2VL} & \theta = 0 \end{cases} \quad (16)$$

and note that M is always nonnegative, then Eq. 15 can be written as

$$r_1 = \Pr\{q_m < (b_1 - x_0)M\} \quad (17)$$

Similarly, the recovery of any type of particle to the right-side bin equals the probability of the particle position at the bottom being greater than b_2, that is

$$r_2 = \Pr\{q_m > (b_2 - x_0)M\} \quad (18)$$

Note that q_m, $(b_1 - x_0)$, and $(b_2 - x_0)$ are all random variables, and that we need only examine the case for $q_m < (b_1 - x_0)M$, since the other case can be found by subtraction. Assuming the particle charge to mass ratio is normally distributed with mean μ and standard deviation σ, and the displacement $(b_1 - x_0)$ is uniformly distributed from $b_1 - a$ to $b_1 + a$, we have

$$Z = q_m \sim N(\mu, \sigma) \quad \text{and} \quad Y = (b_1 - x_0) \sim U(b_1 - a, b_1 + a) \quad (19)$$

From Figure 4, the probability can be computed as

$$\Pr(Z < YM) = F(M) = \int_{b_1 - a}^{b_1 + a}\int_{-\infty}^{yM} f_{yz}(y,z)\, dz\, dy \quad (20)$$

where f_{yz} is the joint probability density function of Z and Y, which is simply the product of their respective probability

Table 3. Conditions for the Nine Cases

	t_1	t_2	t_3	t_4
Case (a)	+	+	−	−
Case (b)	+	−	−	−
Case (c)	−	−	−	−
Case (d)	+	+	+	−
Case (e)	+	−	+	−
Case (f)	−	−	+	-
Case (g)	+	+	+	+
Case (h)	+	−	+	+
Case (i)	−	−	+	+

density functions, since they are independent

$$f_y = \frac{1}{2a}, \quad f_z = \frac{1}{\sqrt{2\pi}\,\sigma} e^{-1/2((z-\mu)/\sigma)^2} \quad \text{and}$$

$$f_{yz} = \frac{1}{2\sqrt{2\pi}\,a\sigma} e^{-1/2((z-\mu)/\sigma)^2} \tag{21}$$

The integral gives:

the recovery to the left-side bin

$$r_{1,l} = \frac{1}{2} + \frac{\Psi(g_2) - \Psi(g_1)}{2(g_2 - g_1)} \tag{22}$$

the recovery to the right-side bin

$$r_{1,r} = \frac{1}{2} - \frac{\Psi(g_4) - \Psi(g_3)}{2(g_4 - g_3)} \tag{23}$$

the recovery to the middle bin

$$r_{1,m} = \frac{\Psi(g_4) - \Psi(g_3) - \Psi(g_2) + \Psi(g_1)}{2(g_2 - g_1)} \tag{24}$$

where

$$g_1 = \frac{M(b_1 - a) - \mu}{\sqrt{2}\,\sigma} \qquad g_2 = \frac{M(b_1 + a) - \mu}{\sqrt{2}\,\sigma}$$

$$g_3 = \frac{M(b_2 - a) - \mu}{\sqrt{2}\,\sigma} \qquad g_4 = \frac{M(b_2 + a) - \mu}{\sqrt{2}\,\sigma} \tag{25}$$

and

$$\Psi(x) = x \cdot erf(x) + e^{-x^2}/\sqrt{\pi} \tag{26}$$

The recovery model for design(d)

The derivation for this part is lengthy, so we only show the important results in this section and readers are welcome to contact the authors for a detailed derivation.

Before applying Eq. 20 to the second stage, the particle charge distribution of the middling from the first stage is derived as follows

$$\frac{\left\{\min\left[\max\left(\frac{Z/M_1 - (b_1 - a)}{(b_1 + a) - (b_1 - a)}, 0\right), 1\right] - \min\left[\max\left(\frac{Z/M_1 - (b_2 - a)}{(b_2 + a) - (b_2 - a)}, 0\right), 1\right]\right\} \frac{e^{-1/2((Z-\mu)/\sigma)^2}}{\sqrt{2\pi}\,\sigma}}{r_{1,m}} \tag{27}$$

where $r_{1,m}$ is the recovery to the middle bin at the first stage (Eq. 24).

Now let the second stage feeder width be $2c$ and the collection bin positions be d_1 and d_2. Let Z represent the distribution by Eq. 27 and Y is the uniform distribution within $(d_1 - c,\ d_1 + c)$. Depending on how the line $Z = YM_2$ intersects with three different density regions, there are nine cases (refer to Table 3). For the first case, we have the following recovery models

the recovery to the left-side bin

$$\frac{\{(g_3 - g_1)[\Psi(h_2) - \Psi(h_1)] - (h_2 - h_1)[\Psi(g_3) - \Psi(g_1)]\}}{2(g_2 - g_1)(h_2 - h_1)r_{1,m}} \tag{28}$$

the recovery to the right-side bin

$$1 - \frac{(g_3 - g_1)[\Psi(h_4) - \Psi(h_3)] - (h_4 - h_3)[\Psi(g_3) - \Psi(g_1)]}{s(g_4 - g_3)(h_4 - h_3)r_{1,m}} \tag{29}$$

where, h is defined as below

$$h_1 = \frac{M_2(d_1 - c) - \mu}{\sqrt{2}\,\sigma} \qquad h_2 = \frac{M_2(d_1 + c) - \mu}{\sqrt{2}\,\sigma}$$

$$h_3 = \frac{M_2(d_2 - c) - \mu}{\sqrt{2}\,\sigma} \qquad h_4 = \frac{M_2(d_2 + c) - \mu}{\sqrt{2}\,\sigma} \tag{30}$$

The complete recovery model for the second stage is shown in Table 4.

Optimizing the Designs and Operations

For the design of electrostatic separators, the degrees of freedom are:

(1) Plate length: L (m);
(2) Feed gap between plates: d (m);
(3) Plate angle: θ;
(4) Feeder opening: $2a$ (m);
(5) Collection-bin positions: b_1 and b_2 (m);
(6) Voltage: V (V);
(7) Plate width: W (m);
(8) Recycle rate: R (between 0 and 1, for design (b) only).

The complete optimization model for one-stage (no recycle) separators is shown in Table 5. The cost models and the capacity constraint were developed from industrial data (Yan, Outokumpu Technology Inc., personal communication). For the objective function that is the maximization of the total profit, the first term is the revenue from selling recycled products, the second term represents the annual unit capital

Table 4. The Recovery Models for the Second Stage*

Case (a)	$\dfrac{\{(g_3-g_1)[\Psi(h_2)-\Psi(h_1)]-(h_2-h_1)[\Psi(g_3)-\Psi(g_1)]\}}{2(g_2-g_1)(h_2-h_1)r_{1,m}}$
Case (b)	$\dfrac{\left\{(g_3-g_1)\Psi(h_2)+(h_2-h_1)\Psi(g_1)+g_1-\Psi(h_1)-h_2\Psi(g_3)+\dfrac{erf(h_1)-\mathrm{erf}(g_3)}{2}\right\}}{2(g_2-g_1)(h_2-h_1)r_{1,m}}$
Case (c)	$\dfrac{\left\{(g_3-g_1)\Psi(h_2)+h_2[\Psi(g_1)-\Psi(g_3)]+\dfrac{\mathrm{erf}(g_1)-\mathrm{erf}(g_3)}{2}\right\}}{2(g_2-g_1)(h_2-h_1)r_{1,m}}$
Case (d)	$\dfrac{(g_3-g_1)[\Psi(h_2)-\Psi(h_1)]-(h_2-h_1)[\Psi(g_3)-\Psi(g_1)]+g_2\Psi(h_2)-h_2\Psi(g_2)+\left[\dfrac{\mathrm{erf}(h_2)-\mathrm{erf}(g_2)}{2}\right]}{2(g_2-g_1)(h_2-h_1)r_{1,m}}$
Case (e)	$\dfrac{g_1\Psi(h_1)-h_2\Psi(g_3)+g_4\Psi(h_2)-h_2\Psi(g_2)+(h_2-h_1)\Psi(g_1)+\dfrac{\mathrm{erf}(h_1)-\mathrm{erf}(g_2)-\mathrm{erf}(g_3)+\mathrm{erf}(h_2)}{2}}{2(g_2-g_1)(h_2-h_1)r_{1,m}}$
Case (f)	$\dfrac{h_2\Psi(g_1)-h_2\Psi(g_3)+g_4\Psi(h_2)-h_2\Psi(g_2)+\dfrac{\mathrm{erf}(g_1)-\mathrm{erf}(g_2)-\mathrm{erf}(g_3)+\mathrm{erf}(h_2)}{2}}{2(g_2-g_1)(h_2-h_1)r_{1,m}}$
Case (g)	$\dfrac{h_2[\Psi(g_1)-\Psi(g_2)-\Psi(g_3)+\Psi(g_4)]+[h_1\Psi(g_3)-g_3\Psi(h_1)+g_1\Psi(h_1)-h_1\Psi(g_1)]-\dfrac{\mathrm{erf}(g_2)-\mathrm{erf}(g_4)}{2}}{2(g_2-g_1)(h_2-h_1)r_{1,m}}$
Case (h)	$\dfrac{h_2[\Psi(g_1)-\Psi(g_2)-\Psi(g_3)+\Psi(g_4)]+[g_1\Psi(h_1)-h_1\Psi(g_1)]+\dfrac{\mathrm{erf}(h_1)-\mathrm{erf}(g_2)-\mathrm{erf}(g_3)+\mathrm{erf}(g_4)}{2}}{2(g_2-g_1)(h_2-h_1)r_{1,m}}$
Case (i)	$\dfrac{h_2[\Psi(g_1)-\Psi(g_2)-\Psi(g_3)+\Psi(g_4)]+\dfrac{\mathrm{erf}(g_1)-\mathrm{erf}(g_2)-\mathrm{erf}(g_3)+\mathrm{erf}(g_4)}{2}}{2(g_2-g_1)(h_2-h_1)r_{1,m}}$

*Left-side bin.

Table 5. Model for Optimizing One-Stage (No Recycle) Separators

Objective

$$\max[C_0F_0(s^Af_0^Ar_1^A+s^Bf_0^Br_2^B)]-\frac{1}{Depn}[C_1+C_2\times(WL)^{0.6}]-[C_0\times C_4\times C_3\times(WLV^2)]$$

Constraints

1. Recovery model: Eqs. 22 and 23
2. Product purity requirement: ≥ 0.995
3. Upper bound on capacity F_0: $F_0 \leq 5215.8(Wd)-1055.8$
4. Design specifications:
   - Plate length: $0.9 \leq L \leq 2$
   - Plate gap: $d \geq 0.3$
   - Plate angle: $0 \leq \theta \leq 15°$
   - Plate width: $0.6 \leq W \leq 1.5$
   - Ratio of gap to length: $d \leq L/3$
   - Voltage: $V \leq 80$ kV

Notation

F_0	Feed rate (kg/h)
f_0^A, f_0^B	Initial fraction of type A and B plastics in the feed
s^A, s^B	Prices of two types of plastics
r_1^A, r_2^B	Recoveries of type A and B particles to left and right bins, respectively
C_0	Coefficient used to convert the units from hour to year. In this case, it is 1600, based on 8 hr/day and 200 days/yr
C_1	Fixed investment cost of the unit (= \$26,060)
C_2	Coefficient for the variable design cost (= \$73,690)
C_3	Coefficient for energy consumption ($= 4e-9$)
C_4	Electricity price (= \$0.06/kWh)
Depn	Number of years depreciation (= 5 yr)

cost, which is assumed to be a function of plate area LW, and the third term is the operating cost (energy consumption), which is a function of plate area (LW) and the voltage, V. For the third constraint, it is assumed that each slice (with width ΔW and gap Δd) of the separator has constant capacity. Therefore, the linear relationship of the flow rate and the feed area (Wd) of the separator was developed.

It is easy to modify the model in Table 5 for the other design options. For design (b), the feed rate F_0 is replaced by the sum of the fresh feed rate and the flow rate in the recycle, which is the product of the recycle rate and the middling rate. For design (c), the unit capital cost and operating cost are the sum of two separators, respectively; the feed flow rate and composition for the second separator are the same as those in the middling of the first stage, respectively; the charge distribution of the feed to the second stage is the same as that in the first stage. For design (d), the objective function is the same as in option (c), except that there is no cost for the charging device for the second stage. The recovery model for various scenarios is shown in Table 4 and the feed flow rate, composition and charge distribution are the same as those in the middling of the first stage.

The preceding models were optimized using AMPL, which is a mathematical programming language developed by Fourer et al. (1993) and SNOPT 5.3.4, which is a nonlinear optimization solver developed by Gill et al. (1997) under various feed flow rates, charge mean values, and standard deviations. The initial feed ratio was chosen to be 50/50, and the two types of particles are assumed to have the same absolute value of charge mean and the same standard deviation. Different design options are compared and analyzed below.

Parallel vs. diverging plates

For the various conditions considered in this article, a parallel-plate design is always better than the diverging one (that is, angle $\theta = 0$), since the latter has a weaker electrical field and there are no compensating advantages. However, some industrial designs do use diverging plates to alleviate the rebound of particles after they collide with the walls. The issue was neglected in this article by assuming the walls were inelastic. Since the angle is usually small in these industrial designs, the angle should not have any influence on the following comparisons of various design options.

Influence of particle mean charge (the unit is μC/kg for all figures below) and standard deviation on design choices

1. Design (a) vs. Design (b). The profit ratio is a normalized objective value that is defined as the ratio of the objective value of the design to that of the reference design indicated in the captions of Figures 5–8. From Figure 5a, the difference is small when the standard deviation is small or high; however, recycling becomes preferable when the standard deviation is in a moderate range. The difference is small at low standard deviation because the recovery is good and the amount in the recycle is too small to make any significant difference; the difference is small at high standard deviation because the particles in the middling are not separable, hence, recycling does not help to improve the overall recovery. The product prices and feed flow rate do not have much influence on the preceding conclusion. From Figure 5b, the recycle rate

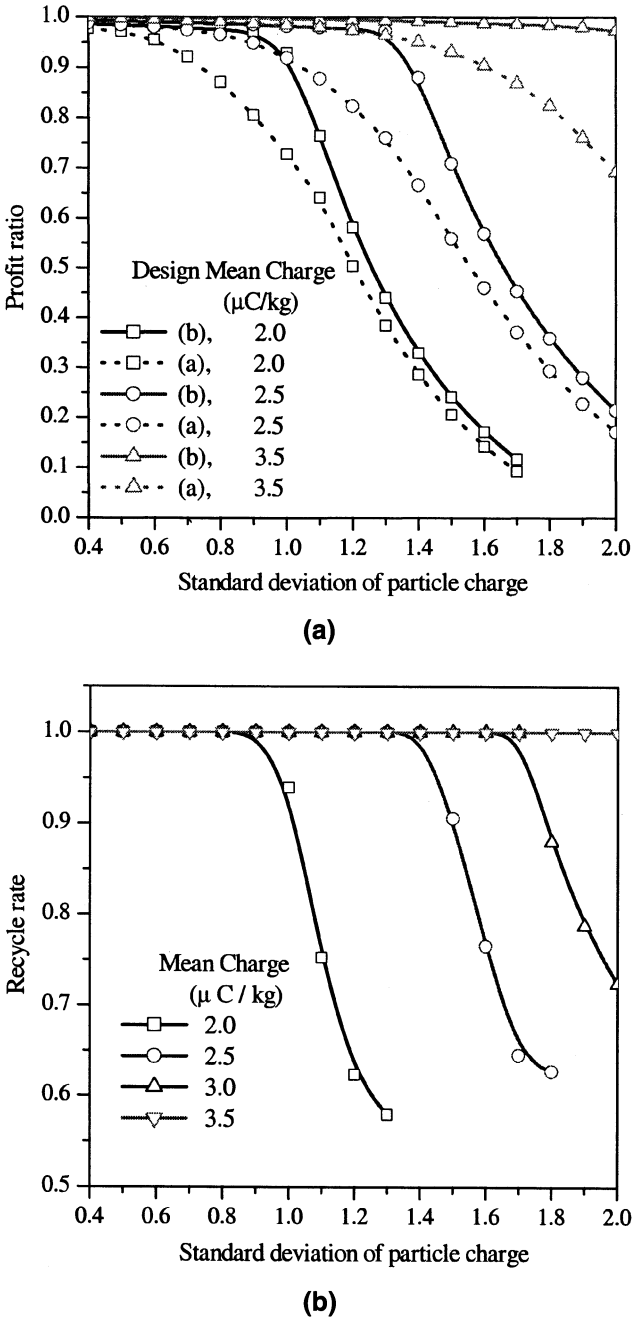

Figure 5. (a) Comparison of design option (a) and (b) at feed flow rate 1,000 kg/h and product prices 0.4/0.4 $/kg [the reference design is design (b) at mean charge 3.5 μC/kg and standard deviation 0.4]; (b) effect of charge mean and standard deviation on the recycle rate at the same condition as in part (a).

is one when the standard deviation is small and then decreases with the standard deviation; as the mean charge increases, the range of the standard deviation at which the recycle rate is one is larger. The recycle rate decreases because the particles in the recycle become more inseparable and the amount of the middling is larger due to the increased number of particles with overlapping charges.

2. Design (a) vs. Design (d). From Figure 6a, one-stage separation is always better than two-stage separation, since the revenue from recovering more particles by adding one more stage is not high enough to cover the cost of the second stage. As the mean charge increases, the objective value is more robust to the variation of the standard deviation of charges (curve becomes flatter). Initially, two-stage separation results are the same as one-stage separation because one stage is enough to recover all particles. As the standard deviation of particle charge increases, there is a transition point, where one stage is not enough to recover all particles, and the second stage starts to take effect.

Figure 6b represents a higher feed flow rate. Two-stage separation may be better than one-stage separation at a moderate standard deviation of particle charges. At mean charge 2.0 μC/kg, two-stage separation is better than one-stage separation for a standard deviation of particle charge between 0.7 and 1.2. The first standard deviation value (0.7) repre-

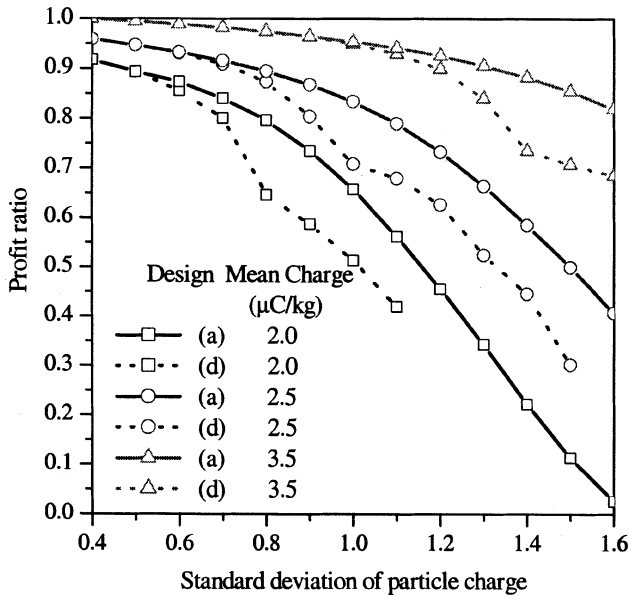

(a)

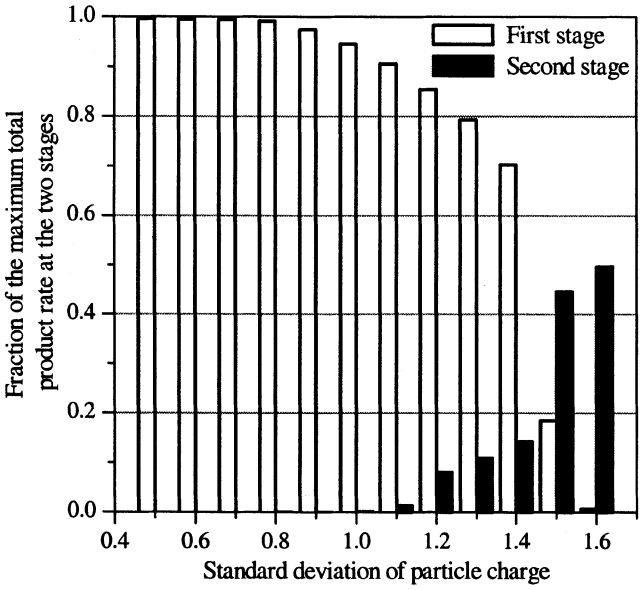

(c)

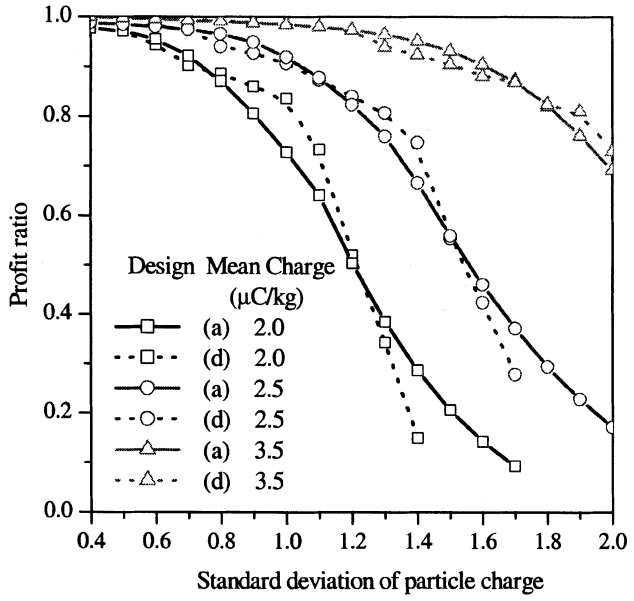

(b)

Figure 6. (a) Comparison of design (a) and design (d) at feed flow rate 200 kg/h and product prices 0.4/0.4 $/kg [the reference design is the design (a) at mean charge 3.5 μC/kg and standard deviation 0.4]; (b) comparison of design (a) and design (d) at feed flow rate 1,000 kg/h and product prices 0.4/0.4 $/kg [the reference design is the design (a) at mean charge 3.5 μC/kg and standard deviation 0.4]; (c) product weight recovered by each stage (for design d) at flow rate 1,000 kg/h and product prices 0.4/0.4 $/kg (at mean charge 2.5 μC/kg, the maximum total product rate is 1,000 kg/h).

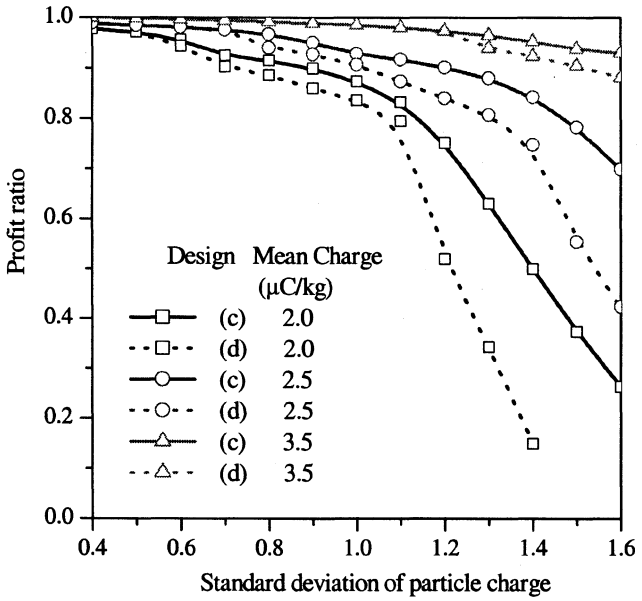

Figure 7. Comparison of two-stage separations (no recharge vs. recharge) at feed flow rate 1,000 kg/h and product prices 0.4/0.4 $/kg [the reference design is the objective value of design (c) at mean charge 3.5 μC/kg and standard deviation 0.4].

sents a transition at which the revenue from recovered plastics from the second stage just covers the cost of the second stage. At standard deviations lower than this value, the one-stage separation is better than two-stage separation because one-stage can provide enough recovery so the cost of the second stage exceeds the added revenue. The second standard deviation value (1.2) represents another transition at which the recovery at the second stage becomes poor, and again the revenue from recovered plastics just balances the cost of the second stage. At standard deviations higher than this value, one-stage separation is better than two-stage separation because particles fed to the second stage are almost inseparable, so additional stages do not help to improve the overall recovery. As the mean charge increases, the transition points shift toward higher standard deviation values.

By comparing the fraction of the product rate recovered by each stage of design (d), the relative contribution of each stage to the overall recovery can be seen. From Figure 6c, at high standard deviation of particle charge (> 1.5), the second stage recovers more particles than the first stage does. At the second stage, with the same voltage, the plates are generally longer or more narrowly separated than the first stage, which means a stronger electrical field and longer separation time. This explains why the second stage is able to separate particles from the middling of the first stage without recharging them.

3. Design (c) vs. Design (d). From Figure 7, the two design options provide similar results at low standard deviation. If the charging process is expensive, the two-stage separation without recharging is preferable. As the standard deviation increases, the second stage without recharging is not of much help in separating the particles, so two-stage separation with recharging is better. Therefore, recharging is preferable only at a high standard deviation. The product prices and feed flow rate do not have much influence on this conclusion.

A simple guide to the selection of designs under a different particle mean charge and standard deviation

As a summary for the preceding comparisons, Figure 8 provides a general guide for selecting an appropriate design (at high feed flow rate or product prices) under various values of charge mean and standard deviation. The two-dimensional (2-D) space is divided into four regions. In region A, where the standard deviation of the charge is very low, the four designs provide similar results, but design (a) is the least expensive one. In region B, where the standard deviation of particle charge is moderately low, recycling becomes helpful to improve the recovery. In region C, where the standard deviation is moderate, two-stage separations are better than one-stage separation (without recycle), but one-stage separation with recycle is still the best one. In region D, due to the high standard deviation, recycling is not as efficient as adding a second stage with recharging, therefore design (c) is the best one. If the flow rate and product prices are both low, two-stage separations should not be used, and recycling should be used if the standard deviation of particle charges is moderate.

Conclusions

In this article, a general design methodology is presented for free-fall electrostatic separators. First, a trajectory model was derived so that the final position of particles at arbitrary starting location and with arbitrary charge can be computed.

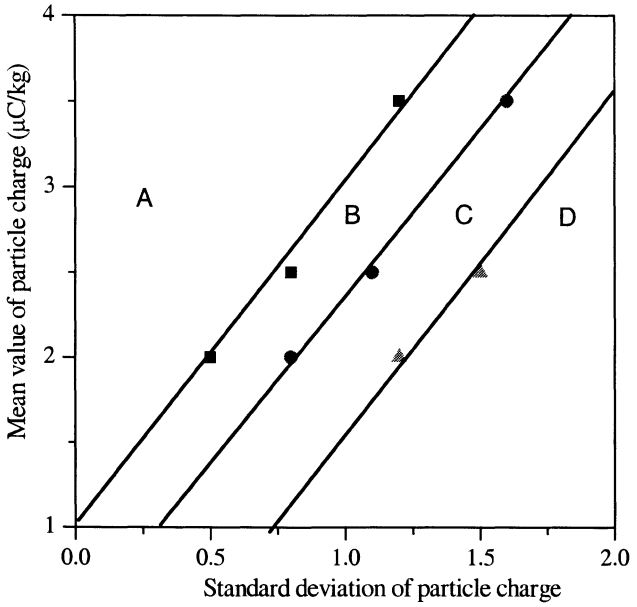

Figure 8. Selection guide for choosing an appropriate design.

Region A: $(a) \approx (b) \approx (c) \approx (d)$; Region B: $(b) > (c) \approx (d) \approx (a)$; Region C: $(b) > (c) > (d) > (a)$; Region D: $(c) > (b) > (a) > (d)$.

Second, the recovery models for four design options were derived based on probability theory. Finally, optimization models with the objective of maximizing the total profit were proposed and the designs were optimized and compared under various flow rates, charge mean values, and standard deviations. Therefore, the models proposed in this article can be used to optimize this class of separators and derive information about the separator size, operating conditions such as the voltage and feed flow rate, and also whether recycling or a second stage (with or without recharging) is helpful.

It was found that a second stage is preferable at high feed flow rate or product prices, and that recharging is helpful if the standard deviation of particle charge is not small. At low feed rate or product prices, recycling is preferable at moderate standard deviation. As a summary, a simple guide for selecting an appropriate design was given.

Although this article is based on free-fall separators, the effect of charge mean and standard deviation on the choice of a different design also may be applicable to the drumtype separators, except that the critical values (for low, moderate, and high values of charge mean and standard deviation) might be different. In future research, the systematic approach (trajectory modeling and recovery modeling) presented in this article will be extended to other trajectory-based separation processes for particles with different densities, sizes, conductivities and polarities, among others, in various fields (electric or magnetic field, liquid/gas flow, and so on).

Acknowledgments

The authors gratefully acknowledge partial financial support by the National Science Foundation, Grant No. 9800198 and the State of Georgia Pollution Prevention Division of the Department of Natural Resources. We thank Dr. John Pelesko of the School of Mathematics for helpful discussions on electrostatics.

Literature Cited

Botsch, M., and R. Köhnlechner, "Electrostatic Separation and Its Industrial Application for the Processing of Different Mixtures of Recycling Materials," *Proc. IMPC-Aachen*, Aachen, Germany, p. 297 (1997).

Fourer, R., D. M. Gay, and B. W. Kernighan, *AMPL, A Modelling Language for Mathematical Programming*, Boyd and Fraser, Danvers, MA (1993).

Gill, P. E., W. Murray, and M. Saunders, *SNOPT: An SQP Algorithm for Large-Scale Constrained Optimization*, Rep. NA 97-2, Dept. of Mathematics, Univ. of California, San Diego, CA (1997).

Higashiyama, Y., Y. Ujiie, and K. Asano, "Triboelectrification of Plastic Particles on a Vibrating Feeder Laminated with a Plastic Film," *J. Electrostatics*, **42**, 63 (1997).

Inculet, I. I., *Electrostatic Mineral Separation*, Research Studies Press, Wiley, New York (1984).

Inculet I. I., G. S. P. Castle, and J. D. Brown, "Electrostatic Separation of Plastics for Recycling," *Part. Sci. Technol.*, **16**, 91 (1998).

Kamptner, A., O. Mientkewitz, and G. Schubert, "The Electrostatic Separation of PVC Containing Waste," *Proc. IMPC-Aachen*, Aachen, Germany, p. 403 (1997).

Kwetkus, B. A., "Particle Triboelectrification and Its Use in the Electrostatic Separation Process," *Part. Sci. Technol.*, **16**, 55 (1998).

Lowell, J., and A. C. Rose-Innes, "Contact Electrification," *Adv. Phys.*, **29**, 947 (1980).

Mihailescu, M., A. Samuila, A. Urs, R. Morar, and A. Iuga, "Computer-Assisted Experimental Design for the Optimization of Electrostatic Separation Processes," *Conf. Record of IAS Annual Meeting*, Vol. 1, IEEE, Piscataway, NJ, p. 687 (2000).

Norbert, R., and S. Ingo, "Tubular Free-Fall Separator for Separating Plastic Mixtures," U.S. Patent No. 5,687,852 (Nov. 18, 1997).

Stahl, I., and P. M. Beier, "Sorting of Plastics Using the Electrostatic Separation Process," *Proc. IMPC-Aachen*, Aachen, Germany, p. 395 (1997).

Vlad, S., A. Luga, and L. Dascalescu, "Modelling of Conducting Particle Behaviour in Plate-Type Electrostatic Separators," *J. Phys. D: Appl. Phys.*, **33**, 127 (2000).

Xiao, C., L. Allen, M. B. Biddle, and M. M. Fisher, "Electrostatic Separation and Recovery of Mixed Plastics, Sixth Ann. Recycling Conf. of the Soc. of Plastics Engineers, Detroit, MI (1999).

Yan, E. S., T. J. Grey, and T. U. Niitti, "Electrostatic Separation Apparatus and Method Using Box-Shaped Electrodes," U.S. Patent No. 6,329,623 B1 (Dec. 11, 2001).

Yanar, D. K., and B. A. Kwetkus, "Electrostatic Separation of Polymer Powders," *J. Electrostatics*, **35**, 257 (1995).

Appendix: The Recovery Model of the Second Stage

Since there are three different density regions (I, II, and III in Figure A1), the recovery integral depends on how the line $Z = YM_2$ intersects the regions. In Figure A1, the three density regions are defined by the Y-values from $d_1 - c$ to $d_1 + c$ and Z-values in region I from $M_1(b_1 - a)$ to $M_1(b_2 - a)$, region II from $M_1(b_2 - a)$ to $M_1(b_1 + a)$, and region III from $M_1(b_1 + a)$ to $M_1(b_2 + a)$, respectively. The integral for the recovery to the left bin covers the density area at the lefthand side of the line $Z = YM_2$. The intersection points of the line $Z = YM_2$ with the top and bottom boundary of the regions have the values $(M_2(d_1 - c), d_1 - c)$ and $(M_2(d_1 + c), d_1 + c)$. The left intersection point can be on the bottom boundary of region II, on the bottom boundary of region I or on the left boundary of region I. Similarly, the right intersection point can be on the top boundary of region II, on the top boundary of region III or on the right boundary of region III. Therefore, there are nine scenarios (that is, a combination of above 3-by-3 cases). We define t_1 as the difference in the Z-values of the left intersection point and the left boundary of region I, t_2 as the difference in the Z-values of the left intersection point and the left boundary of region II, t_3 as the difference in the Z-values of the right intersection point and the right boundary of region II, and t_4 as the difference

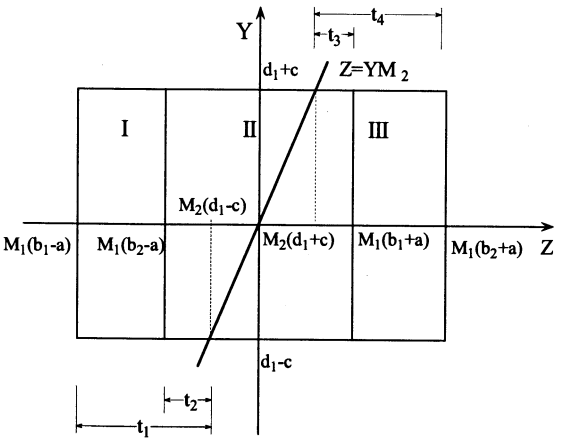

Figure A1. Intersection of the line $Z = YM_2$ and the three density regions.

in the Z-values of the right intersection point and the right boundary of region III. So, we have the following formulas

$$t_1 = M_2(d_1 - c) - M_1(b_1 - a)$$
$$t_2 = M_2(d_1 - c) - M_1(b_2 - a)$$
$$t_3 = M_2(d_1 + c) - M_1(b_1 + a)$$
$$t_4 = M_2(d_1 + c) - M_1(b_2 + a) \qquad (A1)$$

The signs of the t values can be used to describe the conditions for the nine cases (see Table 3). For example, positive t_1 and t_2 and negative t_3 and t_4 represent the case where the two intersection points are on the bottom and top boundaries of region II, respectively (case (a)). Similar conditions (different definitions for t_1, t_2, t_3, t_4; just replace $d_1 + c$ with $d_2 + c$ and $d_1 - c$ with $d_2 - c$) can be constructed for the right-side bin.

Manuscript received Aug. 30, 2002, and revision received Apr. 22, 2003.